

Observation of Dirac-Like Energy Band and Ring-Torus Fermi Surface in Topological Line-Node Semimetal CaAgAs

By using high-resolution angle-resolved photoemission spectroscopy, we experimentally demonstrated that hexagonal pnictide CaAgAs is a new family of topological line-node semimetals exhibiting an ideal bulk-band structure in which a linearly dispersive Dirac-like band solely crosses the Fermi level to form a single line node. Such intriguing spectral signature is in good agreement with our first-principles band-structure calculations that predict a ring-torus Fermi surface and a ring-shaped line node protected by mirror reflection symmetry. The result strongly suggests that CaAgAs provides an excellent platform to study the relationship between low-energy electron dynamics and line nodes in topological semimetals.

Topological semimetals, such as Dirac semimetals (DSMs) and Weyl semimetals (WSMs), have recently attracted particular attention since they exhibit many exotic physical properties such as extremely high mobility, gigantic linear magnetoresistance, and chiral anomaly [1-4]. These physical properties are governed by the Dirac-cone energy band showing linear dispersions in all the momentum (k) directions (k_x , k_y , and k_z), characterized by crossing of the bulk valence band (VB) and conduction band (CB) at discrete points (Dirac points) in k space as seen in Fig. 1(a). Such peculiar electronic structure can be viewed as a sea of massless Dirac or Weyl fermions associated with the protection of band degeneracy by specific symmetries of the crystal.

While DSMs and WSMs are characterized by the crossing of bulk bands at the discrete points in k space (point nodes), there exists another type of topological semimetal characterized by the band crossing along a one-dimensional curve in k space (line node), called line-node semimetal [LNSM; see Fig. 1(a)]. LNSMs are expected to show unique physical properties different from those of DSMs and WSMs, such as a flat Landau level, the Kondo effect, long-range Coulomb interaction, and peculiar charge polarization and orbital magnetism.

Despite many theoretical predictions of LNSMs in various material platforms, there have been relatively few experimental studies on LNSMs.

Recently, it was theoretically proposed by Yamakage *et al.* that noncentrosymmetric ternary pnictides CaAgX ($X = \text{P, As}$) are candidates of LNSMs [5]. These materials crystallize in the ZrNiAl-type structure with space group $P\bar{6}2m$ (No. 189). First-principles band-structure calculations have shown that, under negligible spin-orbit coupling (SOC), CaAgX displays a fairly simple band structure near the Fermi level (E_F) with a ring-like line node (nodal ring) surrounding the Γ point of the bulk hexagonal Brillouin zone (BZ) [bulk BZ is shown in Fig. 1(d)]. The line node is associated with the crossing of bulk CB and VB with Ag s and P/As p character, respectively, and is protected by the mirror reflection symmetry of the crystal. To elucidate the LNSM nature of CaAgX and its relationship to physical properties, we performed high-resolution angle-resolved photoemission spectroscopy (ARPES) of CaAgAs single-crystal [6]. By utilizing variable photons from synchrotron radiation, we established the bulk VB structure in the three-dimensional bulk BZ.

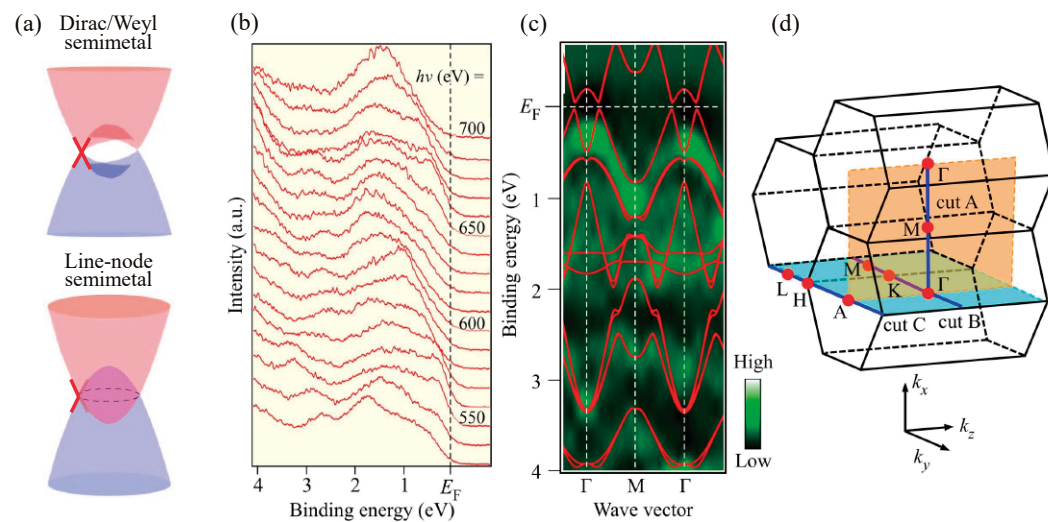


Figure 1: (a) Schematics of Dirac/Weyl semimetal and line-node semimetal. (b) Normal-emission spectra from the $(11\bar{2}0)$ plane of CaAgAs. (c) Band mapping along the Γ M line (cut A) obtained from (b), together with the calculated band dispersions (red curves). (d) Bulk BZ and measured k cuts.

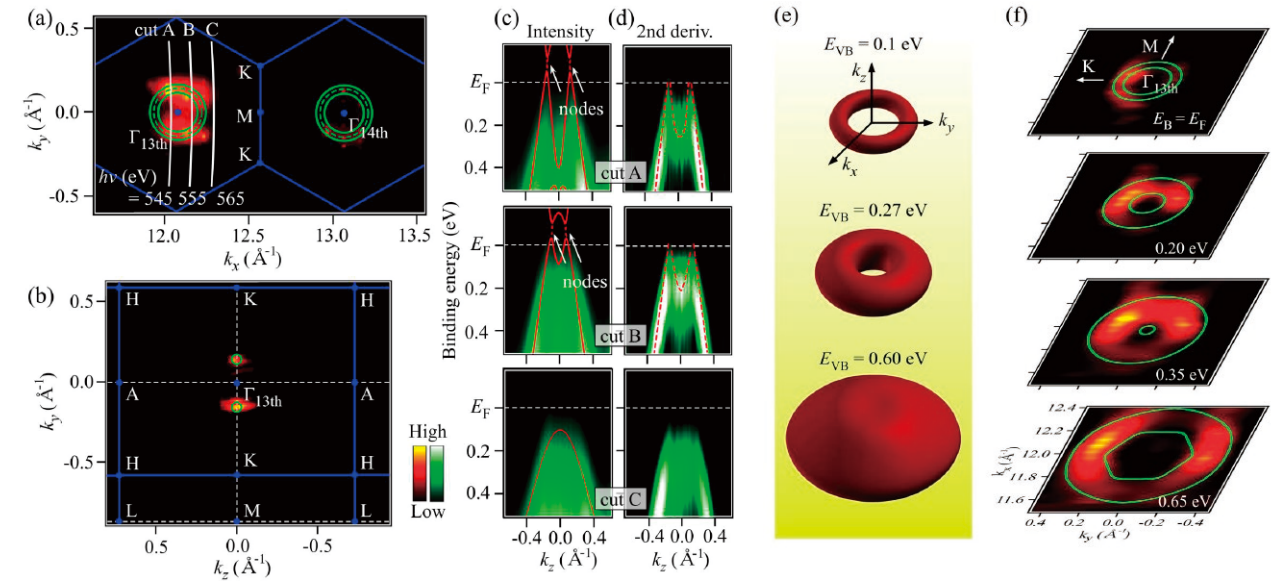


Figure 2: (a), (b) ARPES-intensity mapping at E_F along the Γ KM and Γ AHK planes, respectively. (c), (d) ARPES intensity and second-derivative plot along three representative cuts (cuts A-C in (a)) as a function of E and k . Calculated bands with SOC are shown by solid red curves in (c), while those without SOC are indicated by dashed curves around the node. Dashed red curves in (d) are a guide for the eye. (e) Calculated equi-energy contour maps in k space for selected energy slices. (f) ARPES-intensity mapping for representative E_B slices compared with (e).

Figure 1(b) displays the EDCs at the normal emission measured with various photon energies in the soft X-ray region. To visualize the experimental band dispersion more clearly, we plot in Fig. 1(c) the band structure obtained from the second derivative of the ARPES intensity. One can immediately recognize that the overall experimental band dispersion shows reasonable agreement with the calculated bulk bands (red curves); this confirms that the cleaving plane is $(11\bar{2}0)$. The hole-like dispersion approaching E_F around the Γ point is well reproduced by the calculations, and therefore it is assigned as the topmost VB with the As $4p$ orbital character.

Figure 2(a) and (b) show the ARPES intensity at E_F along the Γ KM and Γ AHK planes, respectively. A bright intensity pattern surrounding the Γ point can be clearly seen. It is also obvious from Fig. 2(b) that no Fermi surface exists away from Γ . The ARPES intensity pattern closely matches the calculated torus-like Fermi surface (green curves). As seen in Fig. 2(c) and (d), the outer and inner rings of the Fermi surface are composed of hole-like linear dispersion which forms the nodes at $k_y \sim 0.15 \text{ \AA}^{-1}$ under negligible SOC. With hole-carrier doping, the linear dispersion forms a torus-like Fermi surface rather than a nodal ring, as depicted theoretically in Fig. 2(e) as well as experimentally in Fig. 2(f). This observation verifies that the bulk Fermi surface is solely derived from the Dirac-like bands forming a single line node, unlike other examples of LNSMs which contain multiple line nodes and/or additional normal bands crossing E_F . This characteristic is of particular

importance since the excitations from the multiple line nodes and the normal bands would smear out genuine physical properties related to the line node. Thus, the CaAgX family is a promising platform to study the direct interplay among line nodes, low-energy excitations, and transport properties in LNSMs.

REFERENCES

- [1] X. Wan, A. M. Turner, A. Vishwanath and S. Y. Savrasov, *Phys. Rev. B* **83**, 205101 (2011).
- [2] S. M. Young, S. Zaheer, J. C. Y. Teo, C. L. Kane, E. J. Mele and A. M. Rappe, *Phys. Rev. Lett.* **108**, 140405 (2012).
- [3] B. Q. Lv, H. M. Weng, B. B. Fu, X. P. Wang, H. Miao, J. Ma, P. Richard, X. C. Huang, L. X. Zhao, G. F. Chen, Z. Fang, X. Dai, T. Qian and H. Ding, *Phys. Rev. X* **5**, 031013 (2015).
- [4] S. Souma, Z. Wang, H. Kotaka, T. Sato, K. Nakayama, Y. Tanaka, H. Kimizuka, T. Takahashi, K. Yamauchi, T. Oguchi, K. Segawa and Y. Ando, *Phys. Rev. B* **93**, 161112(R) (2016).
- [5] A. Yamakage, Y. Yamakawa, Y. Tanaka and Y. Okamoto, *J. Phys. Soc. Jpn.* **85**, 013708 (2016).
- [6] D. Takane, K. Nakayama, S. Souma, T. Wada, Y. Okamoto, K. Takenaka, Y. Yamakawa, A. Yamakage, T. Mitsuhashi, K. Horiba, H. Kumigashira, T. Takahashi and T. Sato, *npj Quantum Materials* **3**, 1 (2018).

BEAMLINES

BL-2A and BL-28A

S. Souma¹, D. Takane¹, K. Nakayama¹, T. Wada², Y. Okamoto², K. Takenaka², Y. Yamakawa², A. Yamakage², T. Mitsuhashi^{1,3}, K. Horiba³, H. Kumigashira^{1,3}, T. Takahashi¹ and T. Sato¹ (¹Tohoku Univ., ²Nagoya Univ., and ³KEK-IMSS-PF)